International Journal of Enhanced Research in Management & Computer Applications
ISSN: 2319-7471, Vol. 10 Issue 6, June, 2021, Impact Factor: 7.751

Study of Prooxidant Filled Low Density Polyethylene

Zeena P Hamza

Department of Chemistry, Maharaja's College, Ernakulam, Kerala, India 682021

ABSTRACT

To improve the photo degradability of low density polyethylene, various metal oxides [iron oxide, manganese dioxide, titanium dioxide (rutile and anatase grades)] and metal stearates (ferric stearate, manganese stearate, cupric stearate, magnesium stearate, and zinc stearate) have been mixed with it. Mechanical properties, melt flow indices, water absorption, and spectroscopic, thermal, and morphological studies are all part of the research. The effect of metal oxides and metal stearates on the photodegradability of LDPE was assessed by exposing test specimens to a 30 watt shortwave UV lamp for one month and then retrieving them. The tensile strength of the material was measured before and after exposure to ultraviolet light. The presence of metal oxides and metal stearates accelerates the photodegradation of LDPE, according to the study.

INTRODUCTION

In the presence of light, most polymers have a natural tendency to undergo a gradual reaction with atmospheric oxygen, which is known as photodegradation. Photodegradation can help polymers disintegrate quickly into a powdery residue with minimal visual impact [1-3]. Abiotic degradation of photodegraded polyethylene can reduce its molecular mass to the point where it is susceptible to biodegradation [4-6]. Activated molecules are formed in the first step of UV irradiation of polymers, and then various processes such as chain scission, cross-linking, and oxidation take place in subsequent steps [7].

The most common method for making polyethylene ox biodegradable is to add prooxidants [8], which cause abiotic oxidation and lower the molecular mass to levels where the material is vulnerable to microbial attack [9-12]. Transition metal complexes, particularly those in the form of stearates, have a remarkable ability to decompose the hydroperoxides formed during polymer oxidation [13]. UV absorbers include metal oxide polymer additives like TiO2 [14].

Melt mixing was used to make low density polyethylene containing 0.1 and 1% prooxidants, such as metal oxides (iron oxide, manganese dioxide, and titanium dioxide (anatase and rutile grades)) and metal stearates (ferric stearate, manganese stearate, copper stearate, magnesium stearate, and zinc stearate). For one month, these samples were exposed to UV light. The neat LDPE was compared to the prooxidant mixed LDPE in terms of mechanical properties, melt flow characteristics, photodegradability, water absorption, FTIR spectra, thermal properties, and morphology.

RESULTS AND DISCUSSION

Metal oxides as prooxidants

Mechanical properties

Metal oxides have an effect on the mechanical properties of LDPE, as shown in Figures 1.1a.1.1b and 1.1c. Figures show that the stress-strain properties of LDPE containing metal oxides are similar to those of pure LDPE, indicating that the metal oxides have no negative impact on the stress-strain properties of LDPE. Figures show that, when compared to neat LDPE, incorporation of 1 percent ferric oxide produces the least variation in tensile strength among the metal oxides used in this study

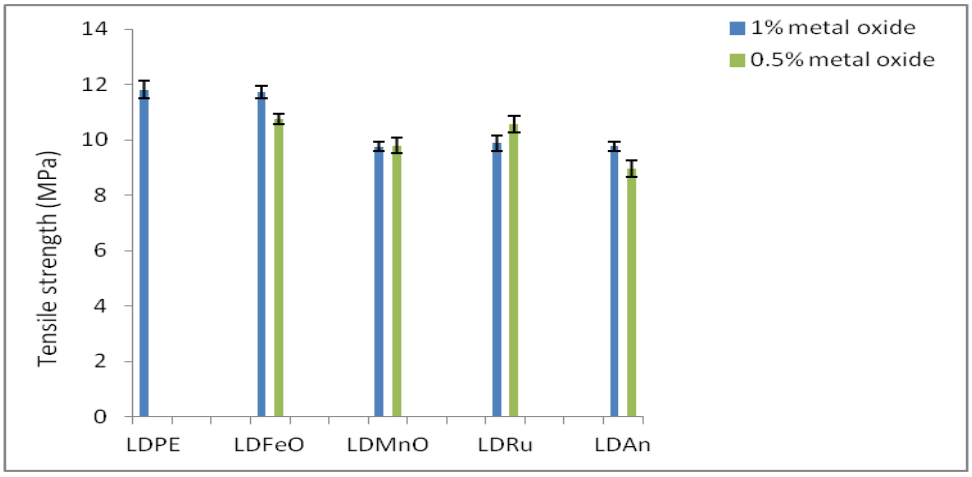

Figure 1.1aEffect of metal oxides on the tensile strength of LDPE

(LDFeO = LDPE-Fe_2O_3, LDMnO = LDPE-MnO_2, LDRu = LDPE-TiO_2 (rutile), LDAn = LDPE-TiO_2 (anatase))

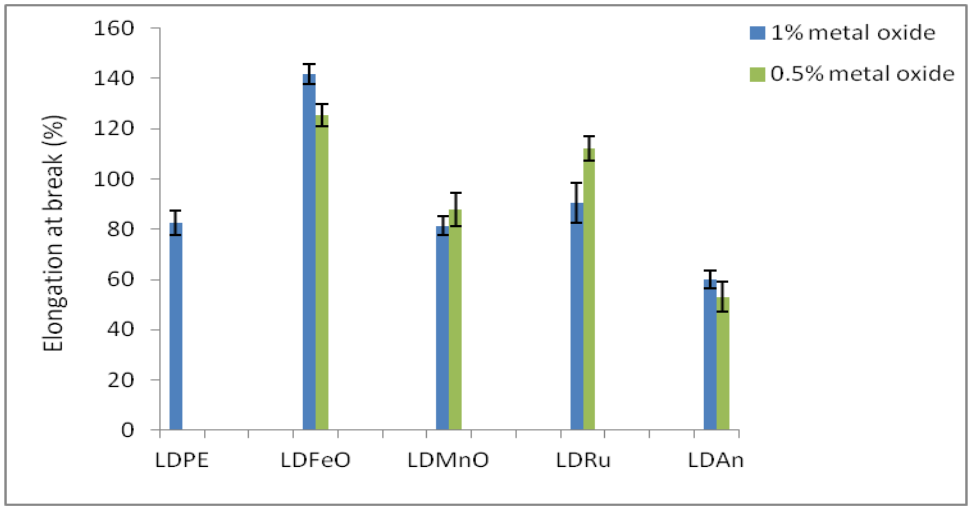

Figure 1.1b Effect of metal oxides on the elongation at break of LDPE

(LDFeO = LDPE-Fe_2O_3, LDMnO = LDPE-MnO_2, LDRu = LDPE-TiO_2 (rutile), LDAn = LDPE-TiO_2 (anatase))

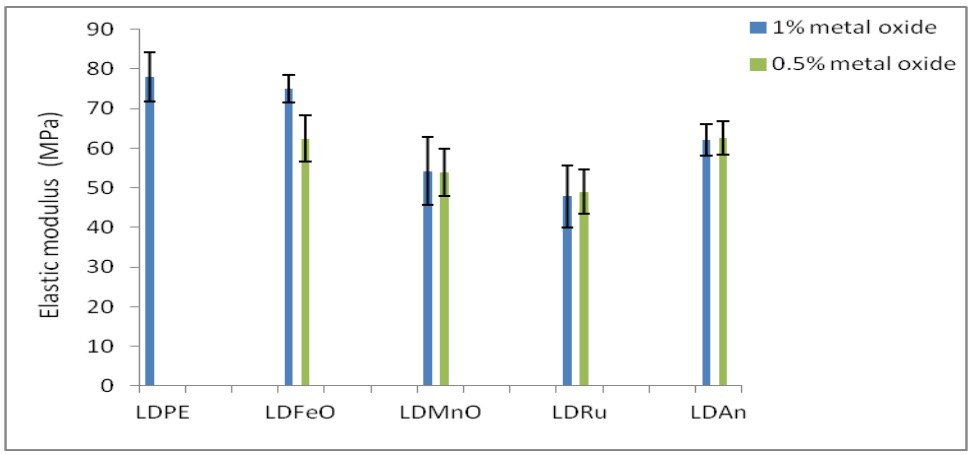

Figure 1.1c Effect of metal oxides on the elastic modulus of LDPE

(LDFeO = LDPE-Fe_2O_3, LDMnO = LDPE-MnO_2, LDRu = LDPE-TiO_2 (rutile), LDAn = LDPE-TiO_2 (anatase))

Melt flow measurements

The met flow rates of neat LDPE and the LDPE-metal oxide mixes are shown in figure 1.2. All the samples except the composition containg MnO_2 show melt flow values almost similar to that of neat LDPE. The results show that processing of LDPE in the presence of these metal oxides does not lead to high level of chain scission or crosslinking so as to cause a change in the melt flow indices [11]. A slight increase in MFI of LDPE containing MnO_2 was observed which indirectly reflects upon the lowering of molecular weight.

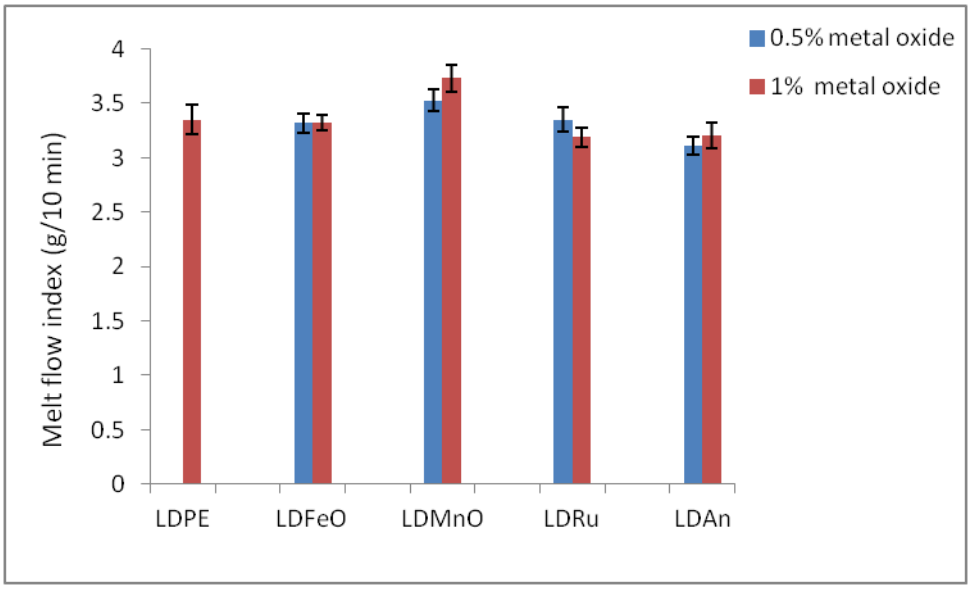

Figure 1.2 Effect of metal oxides on the melt flow index of LDPE

(LDFeO = LDPE-Fe_2O_3, LDMnO = LDPE-MnO_2, LDRu = LDPE-TiO_2 (rutile), LDAn = LDPE-TiO_2 (anatase))

Photo degradability studies

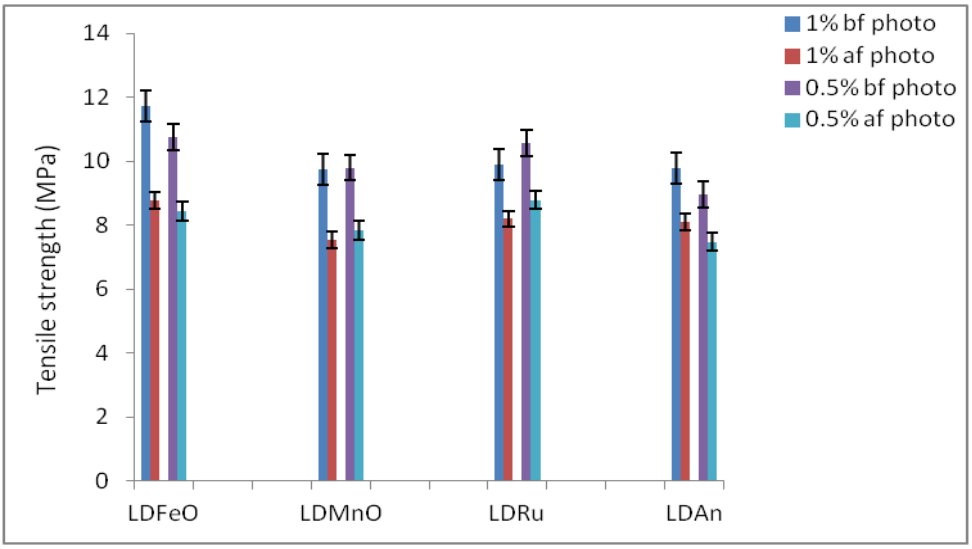

Figure 1.3 Effect of photodegradation on the tensile strength of LDPE containing metal oxides

(LDFeO = LDPE-Fe_2O_3, LDMnO = LDPE-MnO_2, LDRu = LDPE-TiO_2 (rutile), LDAn = LDPE-TiO_2 (anatase))

Figure 1.3 presents the effect of UV exposure for one month on the tensile strength of LDPE containing metal oxides.The tensile strength of all the LDPE-metal oxide compositions decreased after one month of exposure to UV radiation. Among various metal oxides used, the maximum reduction in tensile strength was observed in the case of the film containing 1% Fe_2O_3.Table 1.1 and 1.2 show the loss in tensile strength (%) and loss in weight (%) ofLDPE containing metal oxides after exposure to UV radiation for one month. It was observed that all the samples show a slight rise in weight loss after photodegradation and the weight loss is found to be increases with increase in concentration of metal oxides.

Table 1.1 Percentage decrease in tensile strength of LDPE-metal oxides after UV exposure for one month

Sample	Initial tensile strength (MPa)	Tensile strength after UV irradiation for one month (MPa)	% decrease in tensile strength
LDPE	11.81	11.78	0.21
LD(0.1)FeO	10.71	8.43	21.18
LD(1)FeO	11.72	8.78	21.09
LD(0.1)MnO	9.80	7.83	20.11
LD(1)MnO	9.71	7.14	22.69
LD(0.1)Ru	10.16	8.79	16.76
LD(1)Ru	9.89	8.20	17.09
LD(0.1)An	8.97	7.48	16.61
LD(1)An	9.78	8.10	17.18

(LD(0.1)FeO = LDPE-0.1% Fe_2O_3,LD(1)FeO = LDPE-1% Fe_2O_3, LD(0.1)MnO = LDPE-(0.1)% MnO_2,LD(1)MnO = LDPE-(1)% MnO_2, LD(0.1)Ru = LDPE-0.1% TiO_2 (rutile), LD(1)Ru = LDPE-1% TiO_2 (rutile), LD(0.1)An = LDPE-0.1% TiO_2 (anatase), LD(1)An = LDPE-1% TiO_2 (anatase))

Table 1.2 Percentage weight loss of LDPE-metal oxides after UV exposure for one month

Sample	Initial weight (g)	Weight after one month (g)	% Weight loss
LDPE	0.1181	0.1184	0.02
LD(0.1)FeO	0.1419	0.1412	0.13
LD(1)FeO	0.4492	0.4480	0.27
LD(0.1)MnO	0.4213	0.4209	0.10
LD(1)MnO	0.4790	0.4780	0.21
LD(0.1)Ru	0.4921	0.4923	0.04
LD(1)Ru	0.1992	0.1989	0.01
LD(0.1)An	0.1263	0.1209	1.03
LD(1)An	0.3709	0.3666	1.16

(LD(0.1)FeO = LDPE-0.1% Fe_2O_3,LD(1)FeO = LDPE-1% Fe_2O_3, LD(0.1)MnO = LDPE-(0.1)% MnO_2,LD(1)MnO = LDPE-(1)% MnO_2, LD(0.1)Ru = LDPE-0.1% TiO_2 (rutile), LD(1)Ru = LDPE-1% TiO_2 (rutile), LD(0.1)An = LDPE-0.1% TiO_2 (anatase), LD(1)An = LDPE-1% TiO_2 (anatase))

Water absorption studies

The extent of hydrophilicity of LDPE containing metal oxides was established by % water absorption measurements. The water uptake of the neat LDPE and LDPE-metal oxide compositions are tabulated in Table 1.3. Absence of marginal change in water absorption after 24 hours of immersion in water indicated the hydrophobic character of the blends.

Table 1.3 Water absorption for LDPE and LDPE containing metal oxides

Sample	Initial weight (g)	Weight after 24 hour (g)	% Water absorption
LDPE	0.3337	0.3338	0.03
LD(0.1)FeO	0.2623	0.2628	0.19
LD(1)FeO	0.2394	0.2396	0.08
LD(0.1)MnO	0.2270	0.2271	0.04
LD(1)MnO	0.2247	0.2210	0.13
LD(0.1)Ru	0.2124	0.2121	0.01
LD(1)Ru	0.3112	0.3113	0.03
LD(0.1)An	0.2887	0.2891	0.14
LD(1)An	0.2194	0.2197	0.12

(LD(0.1)FeO = LDPE-0.1% Fe_2O_3,LD(1)FeO = LDPE-1% Fe_2O_3, LD(0.1)MnO = LDPE-(0.1)% MnO_2,LD(1)MnO = LDPE-(1)% MnO_2, LD(0.1)Ru = LDPE-0.1% TiO_2 (rutile), LD(1)Ru = LDPE-1% TiO_2 (rutile), LD(0.1)An = LDPE-0.1% TiO_2 (anatase), LD(1)An = LDPE-1% TiO_2 (anatase))

FTIR spectroscopy

Figure 1.4 shows the changes in the FTIR spectra of LD(1)FeO after exposure to UV for one month.The spectrum shows significant changes in the carbonyl (1781-1700 cm^{-1}), amorphous (1364 cm^{-1}) and hydroxyl regions (3400 cm^{-1}). The absorption peak due to stretching of carbonyl group indicates the presence of numerous oxidation products like H-bonded carboxylic acids (1711 cm^{-1}), esters (1736 cm^{-1}) and γ lactones (1780 cm^{-1})[16-17]. In addition to these bands, absorptions at 1240 and 1410 cm^{-1} are assigned to carboxylic acids and those at 932 and 1640 cm^{-1} are assigned to C=C groups[18].

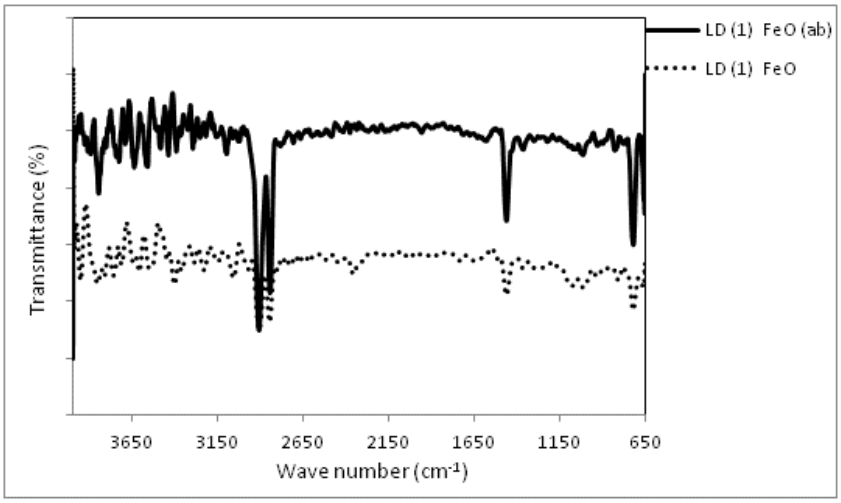

Figure 1.4 FTIR spectra of LD(1)FeO:
a) before degradation b) after degradation

Dynamic mechanical analysis

Figure 1.5 shows the variation in storage modulus and loss factor (tan δ) of LDPE and LDPE containing metal oxides measured over the temperature range from 40^0C to 100^0C. The addition of metal oxides resulted in a shift in the storage modulus curves to higher temperatures, indicating that metal oxide caused a decrease in polymer chain mobility.

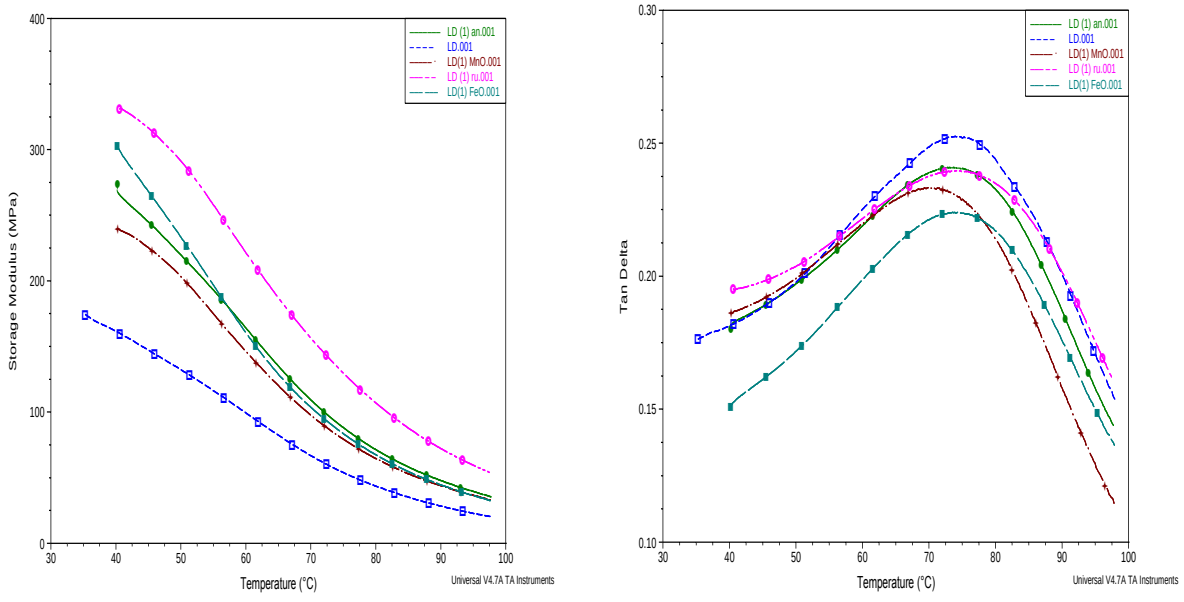

Figure 1.5 DMA spectra of LDPE and LDPE containing 1% metal oxides

Differential scanning calorimetry (DSC)

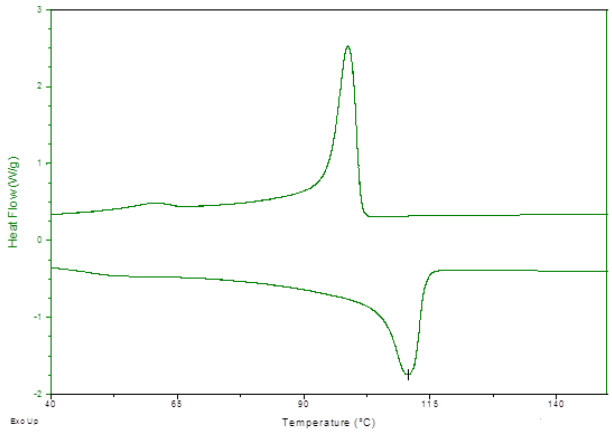

Figure 1.6 DSC thermogram of LD(1)FeO

Figure 1.6 presents the DSC thermogram LD(1)FeO. The melting temperature (T_m), crystallization temperature, heat of fusion, heat of crystallization and the degree of crystallization of pure LDPE and LD(1)FeO were determined and summarized in Table.1.4. For LDPE, the melting point was observed at 110^0C and addition of Fe_2O_3 did not produce any marginal change in melting point. However, the heat of transitions increase upon the addition of Fe_2O_3, which is indicative of increased crystallinity. An increase in crystallinity observed for the blend, is due to the decrease of the polymer chains preferably the amorphous region, and the rearrangement of these molecules causing a larger organization of the chains and thus increasing the region of crystalline material [20].

Table 1.4 Results of DSC analysis of LDPE and LDPE containing 1% ferric oxide

Sample	T_m (^{0}C)	ΔH_f (J/g)	T_c (^{0}C)	ΔH_c(J/g)	% Crystallinity
LDPE	110	67	96	79	23.4
LD(1)FeO	110.13	89.21	98.72	80	31.1

Morphological studies

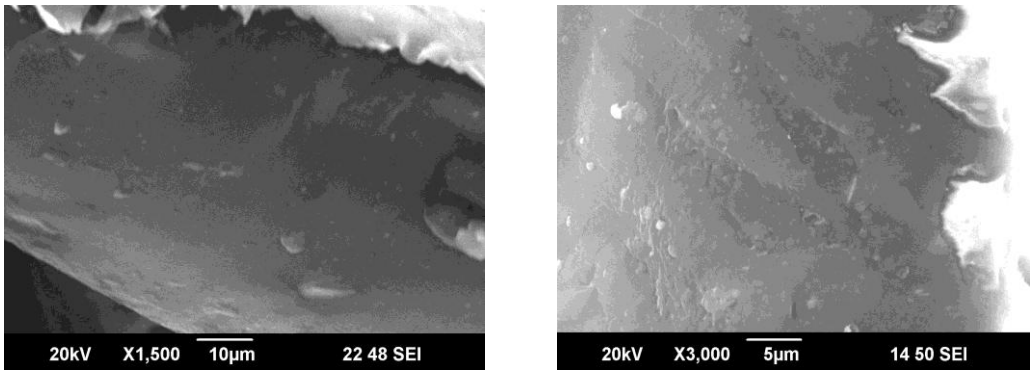

(i) **(ii)**

Figure 1.7 Scanning electron photo-micrographs of LD(1)FeO:
(i) before degradation (ii) after degradation

Figure 1.7 shows the SEM photomicrographs of LD(1)FeO before and after UV exposure for one month. As is apparent from figure the surface of nondegraded film is smooth, without cracks and free from defects. SEM micrographs of the sample after UV irradiation showed grooves and pits indicating that ferric oxide enhance the degradation of LDPE.

CONCLUSIONS

Photodegradation of polyethylene and polyethylene loaded with prooxidant was investigated. Metal oxides and metal stearates are used as the prooxidants. It was observed that LDPE containing prooxidants exhibit mechanical properties in the same range of pure LDPE. All the samples containing metal oxides exhibit an MFI value of ~3-3.1 g/10 min, but in the presence of metal stearates, LDPE shows an increase in MFI values.After photodegradation the tensile strength is found to decrease for mixes of both metal oxides and metal stearates. Spectroscopic studies reveal the presence of oxidation products after degradation. For all the samples, the addition of prooxidants increased the storage modulus, indicating the stiffening imparted by them. There is an enhancement in crystallinity on prooxidant addition.SEM

micrographs of LDPE containing ferric oxide and ferric stearate reveal the presence of weaker points after UV exposure.

REFERENCES

[1]. Gilead, D.; PolymDegrad Stab 1990, 29, 61.
[2]. Jakubowicz, I.; PolymDegrad Stab 2003, 80, 39.
[3]. Wiles, D. M.; Scott, G.; PolymDegrad Stab 2006, 91, 92.
[4]. Albertsson, A. C.; Barenstedt, C.; Karlsson, S.; Lindburg, T.; Polymer 1991, 36, 83.
[5]. Hasan, F.; Shah, A. A.; Hameed, A.; Ahmed, S.; J Appl Polym Sci 2007, 101, 70.
[6]. Weiland, M.; Daro, A.; David, C.; PolymDegrad Stab 1991, 48, 89.
[7]. Tse, K. C. C.; Ng, F. M. F.; Yu, K. N.; PolymDegrad Stab 2006, 91, 2380.
[8]. Roy, P. K.; Surekha, P.; Rajagopal, C.; Choudhary, V.; PolymDegrad Stab 2006, 91, 8.
[9]. Scott, G.; Wiles, D. M.; Biomacromolecules 2001, 2, 22.
[10]. Kyrikou, I.; Briassoulis, D.; J Polym Environ 2007, 11, 10.
[11]. Roy, P. K.; Titus, S.; Surekha, P.; Tulsi, E.; Deshmukh, C.; Rajagopal, C.; PolymDegrad Stab 2008, 93, 22.
[12]. Ojeda, T. F. M.; Dalmolin, E.; Forte, M. M. C.; Jacques, R. J. S.; Bento, F. M.; Camargo, F. A. O.; PolymDegrad Stab 2009, 94, 70.
[13]. Albertsson, A. C.; Barenstedt, C.; Karlsson, S.; Acta Polym 1994, 41, 97.
[14]. Kemp, T. J.; Mclntyre, R. A.; PolymDegrad Stab 2006, 91, 3020.
[15]. Roy, P. K.; Surekha, P.; Raman, R.; Rajagopal, C.; PolymDegrad Stab 2009, 94, 1033.
[16]. Lacoste, J.; Vaillant, D.; Carlsson, D. J.; J Polym Sci A- Chem 1993, 31, 711.
[17]. Wilhelm, C.; Gardette, J. L.; J Appl Polym Sci 1994, 11, 1411.
[18]. Jinguang, W.; Technique and application of advanced Fourier transform infrared spectroscopy, Technological Literature Press, Beijing, 1994, pp. 607-20.
[19]. Pablos, J. L.; Abrusci, C.; Marin, I.; Lopez-Marin, J.; Catalina, F.; Espi, E.; Corrales, T.; PolymDegrad Stab 2010, 91, 2017.
[20]. Sanchez-Solis, A.; Estrada, M. R.; PolymDegrad Stab 1996, 12, 301.
[21]. Koutny, M.; Lemaire, J.; Delort, A. M.; Chemosphere 2006, 64, 12.
[22]. Rivas, B. L.; Seguel, G. V.; Geckeler, K. E.; J Appl Polym Sci 2001, 81, 1310.
[23]. Gulmine, J. V.; Janissek, P. R.; Heise, H. M.; Akcelrud, L.; PolymDegrad Stab 2003, 79, 381.
[24]. Hinsken, H.; Moss, S.; Pauquet, J. R.; Zweifel, H.; PolymDegrad Stab 1991, 34, 279.